

# Magnetic Cellular Automata Wire Architectures

Javier F. Pulecio, *Member, IEEE*, Pruthvi Pendru, Anita Kumari, and Sanjukta Bhanja, *Member, IEEE*

**Abstract**—Magnetic Cellular Automata (MCA) is an unconventional approach to implement Boolean logic machines. Not only has it been able to prototypically demonstrate successful operation of logical gates at room temperature, but it has also realized all the key components necessary to implement any Boolean function. This moves the viability of the technology ahead of other implementations of Cellular Automata (CA), and solicits researchers to examine the various aspects of MCA. Here we investigate a critical facet of the MCA system, the interconnecting wire. We present work further reducing the size of the single domain nano-magnet, approximately  $100 \times 50 \times 30$  nm, and physically implement two types of MCA wire architectures, ferromagnetic and anti-ferromagnetic. We provided external magnetic fields to the systems and investigated the architectures ability to mitigate frustrations. By providing fields in the in-plane easy axis, in-plane hard axis, out of plane hard axis, and a spinning field, we have experimentally concluded that for conventional data propagation between logical networks, ferromagnetic wires provide extremely stable operation. The high order of coupling found under various directions of saturating magnetic fields demonstrates the flexible clocking nature of ferromagnetic wires, and inches the technology closer to implementing complex circuitry.

**Index Terms**—Magnetic Quantum Cellular Automata, QCA, MCA, nano magnets, nano structures, Ferromagnetism

## I. INTRODUCTION

Traditionally, logic circuitry has been wonderfully dominated by the displacement of electric charge. By taking advantage of the predictable tendencies of an electron, we have been able to form immensely complex and dense logic networks that manipulate the "flow" of electrons. Researchers believe that the scaling limit of current transistor technology is near, affording an exciting opportunity for innovation. Scientist and engineers are currently searching for a novel switch to continue increasing the density of logic networks and maintain the trends of smaller more powerful devices. One of the smallest possible switches is the electron itself. Just as electrons possess a fundamental charge, they also have an inherent spin which is naturally discrete. An electron's intrinsic spin and magnetic dipole moment are phenomena that

are redefining the proverbial "box" for logic switches, which has fundamentally been the same for over 50 years.

J. F. Pulecio, P. Pendru A. Kumari and S. Bhanja are with the University of South Florida, Tampa, FL 33612 USA (phone: 813-974-4477; fax: 813-974-5250; e-mail contacts: Javier.Pulecio@gmail.com; bhanja@usf.edu).

Copyright © 2011 IEEE. Personal use of this material is permitted. However, permission to use this material for any other purposes must be obtained from the IEEE by sending a request to pubs-permissions@ieee.org.

Magnetic Cellular Automata (MCA) is a refreshingly novel approach to realize computing machinery by means of a single domain nano magnet as the basic switch. By arranging these nano magnets in a grid like fashion, complex Boolean logic networks can be conceived. With the demonstration of a MCA majority gate, inverter, and interconnecting wire [1], any conceptual Boolean network can be designed. As with any emergent technology, there are stimulating challenges to be transcended. In this paper we present work that augments the understanding of MCA at the device level, by studying wire architectures under the influence of various clocking field.

## II. MCA SYNOPSIS

In MCA, a Boolean state is represented by the orientation of a single domain magnetic dipole moment. In order for MCA to operate, individual magnetic cells must couple through field interactions. There are several different schemes that have been proposed on how to design such a system [2-4]. A principle design was proposed by Cowburn *et al* [2], which experimentally demonstrated data propagation via uniaxial circular nano-magnets at room temperature. It presented a very interesting scheme and can be considered logically synonymous to analog circuitry for MCA. Another significant design was proposed by Csaba *et al* [3], in which the nano-magnets were given more of a digital nature, by introducing shape anisotropy. In this scheme the nano-magnetic cell was engineered in a rectangular shape to create an easy and hard axis of magnetization. This design was experimentally demonstrated [1] and has all the necessary components for the realization of any Boolean logic network, namely, the inverter, majority gate, and interconnecting wire.

## III. MCA WIRE ARCHITECTURES

In order for any logic system to work there must be communication between the various logic components throughout a design. One can observe this at several different levels throughout the design automation process with transistor technology. From individual transistor level to inter-gate signaling or signaling between logical black boxes, the interconnecting wire is fundamental to every aspect of any logic system. Without a means of communicating results from one structure to another, computation is inconsequential. Hence, the reliability of an interconnecting wire providing accurate information is crucial to the functionality throughout a system. In MCA, there have been wire prototypes demonstrating a high order of coupling [5]; encouraged by this, we reproduced similar work and our results indeed verified successful operation [6].

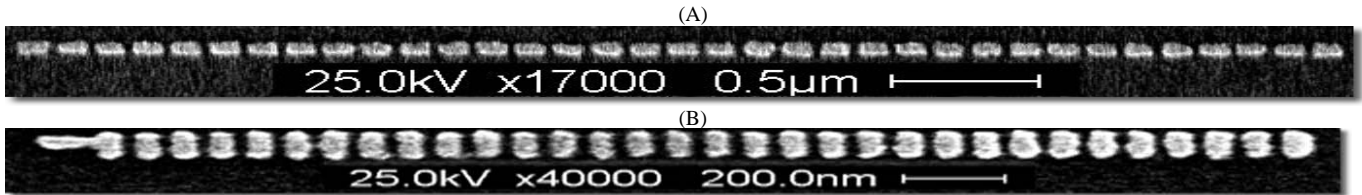


Fig. 1. A SEM image of the (A) ferromagnetic wire and (B) anti-ferromagnetic wire. The dimensions of the nano-magnets were approximately 100 (l) x 50 (w) x 30 (th) nm<sup>3</sup>.

In order to implement complex circuitry, it is necessary to control information propagation of an interconnecting wire via a clock. Researchers have proposed using an adiabatic clocking method that pumps an external magnetic field [7]. The external magnetic clocking field saturates the nano-magnets, causing the overall magnetic dipole moments to align themselves along the in-plane hard axis of the nano structures. The clocking field is reduced as an input is provided. The study of wire architectures under such clocking fields is significant to the advancement of MCA systems.

There are two types of MCA wire architectures that are of particular interest, ferromagnetic wires[4] and anti-ferromagnetic wires[8]. In a ferromagnetic MCA wire, individual nano-magnetic cells are coupled when neighboring cells are aligned in the same direction. For anti-ferromagnetic MCA wires, coupling is exhibited when neighboring magnetic dipole moments are opposing. It is energetically favorable for similar poles to maximize interspatial distances, and therefore, the lowest possible energy for a wire is also the desired configuration for logical computation in a MCA system. There are situations, such as the adiabatic clocking method mentioned above, where similar poles are forced to reduce the interspatial distances. If the magnets settle in this configuration, in order to satisfy local energy minimums, it is known as a magnetic frustration. When a frustration occurs in a wire, the data propagated is erroneous and no longer valid. Therefore, the reliability of a MCA wire lies in the ability to eliminate any magnetic frustrations.

We present the first experimental results comparing shape engineered ferromagnetic and anti-ferromagnetic wires under various magnetic clocking fields. Simulations of the wire architectures were also implemented.

#### IV. FABRICATION AND METROLOGY DETAILS

Fabrication was accomplished via a standard electron beam lithography process [6]. A JEOL 840 SEM retrofitted with the NabyNPGS system operating at 35KV, was used to expose patterns on a Si wafer with a single layer of 950K PMMA resist. A film of 30 nm thick Permalloy was evaporated using a Varian Model 980-2462 Electron Beam Evaporator. Scanning electron microscopy was accomplished with a Hitachi S800SEM. A Digital Instruments Dimension 3100

Scanning Probe Microscope was utilized in two modes for characterization, Atomic Force Microscopy and Magnetic Force Microscopy.

#### V. EXPERIMENTAL SETUP

The specific ferromagnetic and anti-ferromagnetic wires used for the experiment are shown in Fig. 1. The dimension of each nano-magnetic cell was approximately 100 (l) x 50 (w) x 30 (th) nm. The spacing between each cell was approximately 20 nm and the nano-magnets were not annealed. More information about physically relative features can be found here [6]. An electromagnet powered by a 200W regulated dc power supply was used to provide uniform magnetic fields of approximately 200mT (2000 Gauss). The remanent magnetization was recorded via Magnetic Force Microscopy.

The following procedure was used to provide the various external excitations to the magnetic system via an electromagnet. The sample was placed inside of the electromagnet followed by a ramp up period of approximately 2 seconds to 200mT. The sample was left in the saturating field for 5 seconds, followed by a ramp down over 2 seconds.

#### VI. RESULTS AND DISCUSSION

##### A. Experimental Results

In Fig. 2 through 6, the MFM images depict the remanent magnetization of both the ferromagnetic (top) and anti-ferromagnetic (bottom) MCA wires. Each individual magnet has been overlaid with an outline to help interpret results. A blue outline is used to point out an undesired condition, i.e. a frustration.

In Fig. 2, the wires were rotated while inside of the magnetic field, similar to the method used by Bernstein *et al*[9]. The magnetic field was provided to both wire architectures using the procedure outlined in the setup and the nano-magnets were allowed to settle into a ground state. As shown in Fig. 2, there were a few frustrations present in the anti-ferromagnetic wire architecture. Interestingly, the ferromagnetic wire was able to reach the lowest possible energy state with no frustrations present.

In Fig. 3, the magnetic field was provided along the z-axis of the wires. This aligned the magnetic moments in a high energy state due to the shape anisotropy of the nano-magnets. The field was removed and the wires were allowed to settle. It is evident that the number of frustrations present in the anti-ferromagnetic wire architecture increased, whereas the

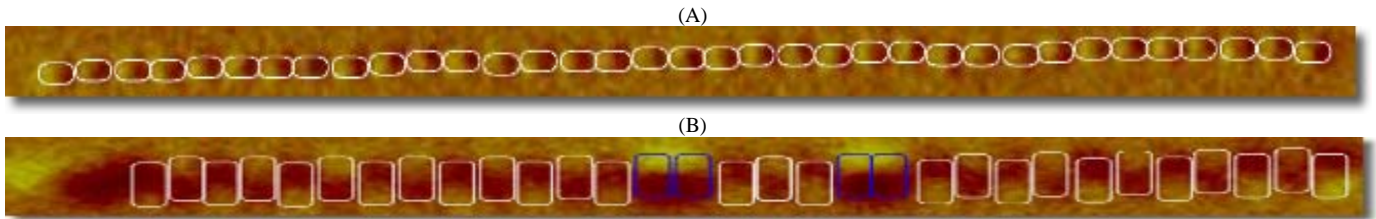


Fig. 2 (Spin magnetic field) A MFM image of (A) the ferromagnetic wire and (B) the anti-ferromagnetic wire. There were very few frustrations in (B) and the ferromagnetic wire has no frustrations.

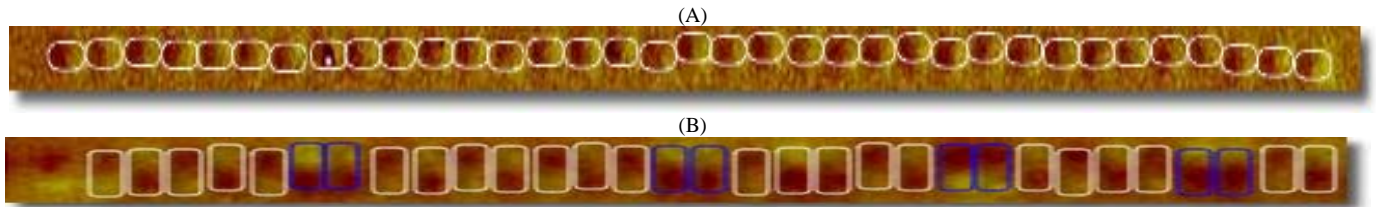


Fig. 3. (Z axis magnetic field) (A) is the ferromagnetic wire and (B) is the anti-ferromagnetic wire. The number of incorrect ordering increased in (B). The ferromagnetic wire had no frustrations.

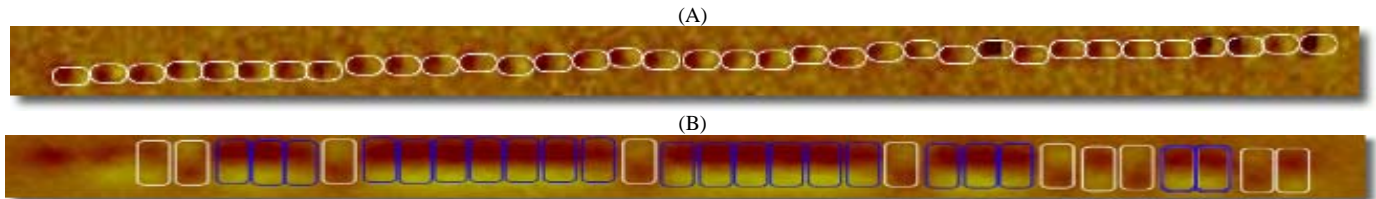


Fig. 4. (Easy axis magnetic field) (A) is the ferromagnetic wire and (B) is the anti-ferromagnetic wire. In (B) there was a significant amount of frustrations. For anti-ferromagnetic wires, this type of clocking field is undesirable. The magnetic moments must overcome the shape anisotropy energy to align in an anti-ferromagnetic fashion. The ferromagnetic wire (A) had no frustrations.

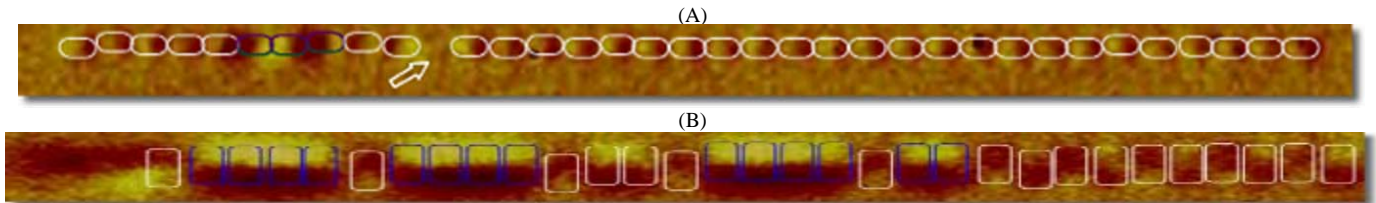


Fig. 5. (Hard axis magnetic field) (A) is the ferromagnetic wire and (B) is the anti-ferromagnetic wire. In (A) an interesting configuration occurred, as pointed out by the arrow. The cell's magnetic dipole moment appeared to be void. It can be seen that the cell was surrounded by like poles, hence forcing the peculiar configuration.

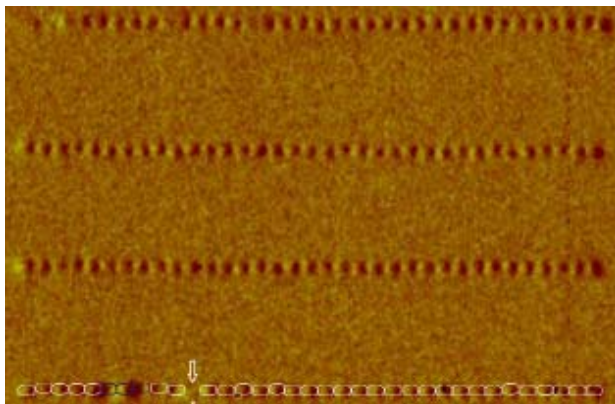


Fig. 6. A hard axis magnetic field was provide to ferromagnetic wires. In this image, the bottom most wire was the same wire shown in Fig 5. Although that particular wire had frustrations, the three neighboring wires above it did not.

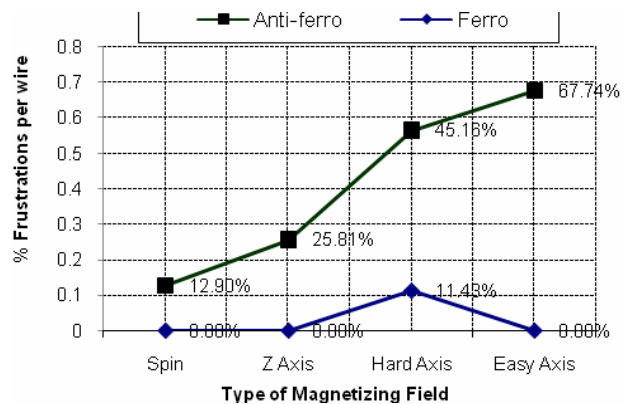


Fig. 7. The graph above summarizes the percentage of frustrations based on the direction of the magnetic field. The field strength for all fields was approximately 200mT (2000 Gauss).

ferromagnetic MCA wire architecture was able to settle with no frustrations.

Similarly, in Fig. 4, a magnetic field was provided along the easy axis of the magnets for both wire architectures. The differences in behavior between the wire architectures become accentuated for this particular field direction. For anti-ferromagnetic wires this is the least desirable type of field to provide. It forces the magnetic moments of each magnet to order in an undesired high energy state. Once the field is removed, the repulsive forces experienced by similar poles must overcome the shape anisotropy energy and align in a more energetically favorable anti-ferromagnetic state. It is clear that the number of frustrations in the anti-ferromagnetic wire architecture is significantly worse (Fig. 4). In the case of the ferromagnetic wire architecture though, this will clearly be the preferred type of field to apply from a magnetic frustration standpoint. Since the applied field lies along the easy axis of magnetization, no frustrations were found in the ferromagnetic wire.

In Fig. 5, the magnetic field was provided along the in-plane hard axis of the nano-magnets. This forced the magnetic moments to align themselves in an unfavorable state due to the shape anisotropy of the nano-magnets. Once the magnetic field was removed, the magnetic moments attempted to align themselves along the easy axis of the nano-magnetic cells. In the anti-ferromagnetic wire, there were several frustrations present. The ferromagnetic wire also showed some susceptibility to magnetic frustrations, with a few undesired states. A very interesting configuration is pointed out by an arrow in Fig. 5. There were two similar poles on either side of the nano-magnet cell and the magnetic moment of the trapped cell was not detected by the microscope. It is possible that the magnetic moment was out of plane and the field was too weak for the MFM to detect.

In Fig. 6, the ferromagnetic wire from Fig. 5 is the bottom most wire. As can be seen in the image, there were three neighboring wires above it. The MFM image shows all three neighboring wires were able to reach a ground state with no magnetic frustrations. The ferromagnetic wire in Fig. 5 did have some frustrations present when providing a field along the hard axis, but neighboring wires did not.

The graph in Fig. 7 summarizes the number of frustrations of both architectures for a given type of applied magnetic field. The experimental data suggested that the ferromagnetic MCA wire architecture is more likely to reach a non-frustrated, and therefore logically correct, ground state.

### B. Simulation Results

The following parameters were used to simulate Permalloy systems via OOMMF; magnetic saturation ( $M_s$ )  $860e3$  A/m, exchange stiffness ( $A$ )  $13e-12$  J/m, and a damping coefficient 0.5. OOMMF solves a given problem by integrating the Landau-Lifshitz equation (Eq. 1), where  $\mathbf{M}$  is the pointwise magnetization,  $\mathbf{H}_{\text{eff}}$  is the effective magnetic field,  $\gamma$  is the gyromagnetic ratio, and  $\alpha$  is the damping coefficient.

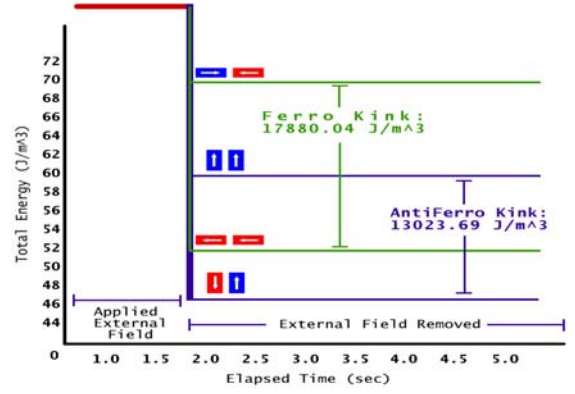


Fig. 8 The graph shows the possible states for the ferromagnetic and anti-ferromagnetic wires and over the duration of the experiments. The higher kink energy for the ferromagnetic wire provides an explanation of its superior ability to mitigate unwanted frustrations.

$$\frac{d\mathbf{M}}{dt} = -|\gamma| \bar{\gamma} |\mathbf{M} \times \mathbf{H}_{\text{eff}} - \frac{|\bar{\gamma}| \alpha}{M_s} \mathbf{M} \times (\mathbf{M} \times \mathbf{H}_{\text{eff}}) \quad (1)$$

$\mathbf{H}_{\text{eff}}$  is calculated in Eq. 2, where  $E$  is the total energy of the system. The total energy  $E$ , calculated in Eq. 3 [10], describes the total average energy density of all the magnetically active elements where;  $E_z$  is the Zeeman energy,  $E_D$  is the demagnetization energy,  $E_{\text{Ex}}$  is the exchange energy, and  $E_A$  is the anisotropy energy.

$$\mathbf{H}_{\text{eff}} = -\mu_0^{-1} \frac{dE}{d\mathbf{M}} \quad (2)$$

$$E = E_z + E_D + E_{\text{Ex}} + E_A \quad (3)$$

The total energy density of all magnetic elements ( $E$ ) from the simulation is highlighted in dark blue in Table 1 for both the desired ground state ( $G$ ) and a metastable state ( $M_s$ ) for anti-ferromagnetic and ferromagnetic architectures. Interestingly, it is worth noting that the total energy of both possible states for the anti-ferromagnetic scheme was lower than the total energy of the equivalent ferromagnetic state. At first glance this would lead one to believe anti-ferromagnetic wires would act more reliably, but this does not capture the observed results. In the experiments above, the ferromagnetic scheme was able to minimize the total number of frustrations and therefore operate in a more reliable manner.

We attribute, but do not limit, the ferromagnetic wires ability to mitigate frustrations more so than the anti-ferromagnetic wires, to the energy difference between the two possible states for the local architectures, also known as the kink energy. The kink energy is defined in Eq. 4 where;  $U_{M_s}$  is the energy associated with the meta-stable (frustrated) state, and  $U_G$  is the energy associated with the desired ground state.

$$E_{\text{Kink}} = U_{M_s} - U_G \quad (4)$$

Fig. 8 shows an abstraction of the experiment where the external magnetic field was given along the z-axis. When the





Architecture States (G=ground, M <sub>s</sub> =metastable)	Exchange Energy (J /m <sup>3</sup> )	Demag Energy (J /m <sup>3</sup> )	Total Energy (J /m <sup>3</sup> )
 (M <sub>s</sub> )	3255.46	56798.92	<b>60054.38</b>
 (G)	3918.31	43112.37	<b>47030.69</b>
 (G)	1365.99	50932.46	<b>52298.45</b>
 (M <sub>s</sub> )	2687.185	67491.31	<b>70178.49</b>

Table 1 The table provides various energies associated with a two nano-magnet ferromagnetic and anti-ferromagnetic system. It captures the two possible states of both schemes, namely the ground state and metastable state.

system was forced to align itself along the z-axis, the total energy was very high, and once the external field was removed both architectures attempt to minimize their local energies. As mentioned above, the total energy of the desired state for the anti-ferromagnetic wire was lower than that of the ferromagnetic wire. Nevertheless, this was not considered by the locally implemented architectures, only the kink energy or the energy between the possible ground and metastable states for the particular architecture was present at the time the external field was removed. As shown in Fig. 2, the kink energy for the ferromagnetic wire was much greater than the anti-ferromagnetic wire; and therefore the ferromagnetic architecture has a higher propensity to mitigate undesired frustrations.

We also attribute the nucleation of frustrations in our experiments in both wire architectures to a multiple driver scenario. Without an input driving the system, it is highly probable for a wire to have multiple drivers. This can be explained by visualizing a wire in a clocked state along the hard axis. Once the magnetic clocking field is removed, any nano-magnetic cell in the chain can become the driver to its neighbor. In fact, multiple drivers can occur throughout a wire, in opposing directions. This leads to magnetic frustrations and is not representative of the ideal operation of a MCA system.

Providing a clocking field along the z-axis of the nano-magnets, where experimentally there were no frustrations found, could also eliminate possible clocking complexities encountered in dense layouts that contain in-plane horizontal and vertical wires.

## VII. CONCLUSION

We have fabricated two types of MCA wire architectures; ferromagnetic and anti-ferromagnetic. By providing clocking fields to the wires, and investigating the remanent magnetic dipole moments, our results show ferromagnetic wires to exhibit exceptional data propagation. We attribute, but do not limit, the ferromagnetic wires' superior ability to mitigate frustrations over the anti-ferromagnetic wires, to the higher kink energy of the ferromagnetic scheme. We note though,

Magnetic Cellular Automata does not have to be limited to just one type of wire architecture per design. Indeed, the ferromagnetic wires could also be mixed with the anti-ferromagnetic wires in the same design. There could be also some circumstances where a particular architecture will be more desirable than the other. Our data suggests that for relatively long data propagation, the ferromagnetic wire architecture will be the preferred implementation for MCA systems.

## ACKNOWLEDGMENT

This work was supported in part by, NSF HRD #0217675, NSF DUE #0807023, NSF CCF #0639624, NSF EMT #0829838, the Alfred P. Sloan fellowship, and the FEF McKnight fellowship.

All fabrication and metrology was done at the University of South Florida's Nano-materials and Nano-manufacturing Research Center. Javier F. Pulecio would like to thank Jay Bieber, Dr. Shekar Bhansali, Dr. Yusuf Emirov, Robert Tufts, and David A. Shears for all the help received throughout various stages of project development.

## REFERENCES

- [1] A. Imre, G. Csaba, L. Ji *et al.*, "Majority logic gate for magnetic quantum-dot cellular automata," *Science*, vol. 311, no. 5758, pp. 205-208, Jan 13, 2006.
- [2] R. P. Cowburn, and M. E. Welland, "Room Temperature Magnetic Quantum Cellular Automata," *Science*, vol. 287, pp. 1466-1468, February, 2000.
- [3] G. Csaba, A. Imre, G. H. Bernstein *et al.*, "Nanocomputing by field-coupled nanomagnets," *Ieee Transactions on Nanotechnology*, vol. 1, no. 4, pp. 209-213, Dec, 2002.
- [4] M. C. B. Parish, and M. Forshaw, "Magnetic Cellular Automata MCA systems," *IEEE Proc-Circuits Devices Syst.*, vol. 151, no. 5, pp. 480-485, October, 2004.
- [5] A. Imre, G. Csaba, G. H. Bernstein *et al.*, "Investigation of shape-dependent switching of coupled nanomagnets," *Superlattices and Microstructures*, vol. 34, no. 3-6, pp. 513-518, Sep-Dec, 2003.
- [6] J. F. Pulecio, and S. Bhanja, "Reliability of bi-stable single domain nano magnets for Cellular Automata." pp. 782-786.
- [7] G. Csaba, W. Porod, and A. I. Csurgay, "A computing architecture composed of field-coupled single domain nanomagnets clocked by magnetic field," *International Journal of Circuit Theory and Applications*, vol. 31, no. 1, pp. 67-82, Jan-Feb, 2003.
- [8] A. Imre, G. Csaba, L. Ji *et al.*, "Majority Logic Gate for Magnetic," *Science*, vol. 311, pp. 205-208, January, 2006.
- [9] G. H. Bernstein, A. Imre, V. Metlushko *et al.*, "Magnetic QCA systems," *Microelectronics Journal*, vol. 36, no. 7, pp. 619-624, Jul, 2005.
- [10] T. L. Gilbert, "A phenomenological theory of damping in ferromagnetic materials," *Magnetics, IEEE Transactions on*, vol. 40, no. 6, pp. 3443-3449, 2004.

**Javier F. Pulecio** was born in Chicago, Illinois, United States of America, in 1982. He received his B.S. in computer engineering from the University of South Florida, Tampa, FL, United States of America, in 2005. Since then, has received his Ph.D. in electrical engineering from the University of South Florida, Tampa, FL, United States of America, in 2010.

In 2005, he worked at Honeywell International Inc. in IR&D of Aerospace and Electronics as Systems Engineer Intern. In the summer of 2008, he was awarded the Graduate Research Internship Program Fellowship (GRIP) at Brookhaven National Laboratories. In 2010, he became a Research Associate at Brookhaven National Laboratories in the department of Condensed Matter Physics & Material Science. His current research interests include nano-

magnetic devices, micro-magnetics, alternative logic devices, nano-lithography and fabrication, characterization of nano-structures, and electron microscopy.

**Pruthvi K. Pendru** was born in Manthani, Andhra Pradesh, India in 1986. He received his B. Tech in Electrical and Electronics Engineering from Jawaharlal Nehru Technological University in Hyderabad, Andhra Pradesh, India in 2007. Since then, has received his Master's degree in Electrical Engineering from the University of South Florida, Tampa, FL, United States of America in 2009.

In 2008, he worked as a Graduate Research Assistant at the University of South Florida. His current research interests include nano-magnetic devices, characterization of nano-magnetic structures and SPM.

**Anita Kumari** received the B.Tech degree in Electronics and Communication Engineering from S.L.I.E.T, India, in 2003 and the M.Tech degree in Microelectronics from Panjab University, Chd, India, in 2005.

She is currently pursuing the Ph.D. degree in Electrical Engineering, in nano research computing group at University of South Florida, Tampa, U.S.A. Her research interests include design and modeling of advance nano-scale devices.

**SanjuktaBhanja** received Bachelor degree in Electrical Engineering from Jadavpur University, Calcutta in 1991 and Master's Degree from Indian Institute of Science, Bangalore in 1994. She finished her PhD degree in Computer Science and Engineering in 2002 from the University of South Florida, Tampa. She is currently an associate professor in the Department of Electrical Engineering at the University of South Florida.

Her primary research focus is in non-CMOS nano-computing, VLSI design automation with emphasis on data-driven uncertainties, trade-off of error, power, and reliability at various levels of design abstractions. She is the recipient of the NSF CAREER award (2007-2012), USF Tau Beta Pi "Outstanding Engineering Faculty Researcher" award, 2007 and USF "Outstanding Faculty Research Achievement Award", 2008, 09/10 Outstanding Undergraduate teaching award, University of South Florida.